VI International Conference on Particle-based Methods – Fundamentals and Applications
PARTICLES 2019
E. Oñate, M. Bischoff, D.R.J. Owen, P. Wriggers & T. Zohdi (Eds)

DEM SIMULATION OF TRIAXIAL TESTS OF RAILWAY BALLAST FOULED WITH DESERT SAND

PABLO JIMÉNEZ[1], JOSÉ ESTAIRE[2], CLARA ZAMORANO[1], ALEJANDRO DE BENITO[1] AND IGNACIO G. TEJADA[1]

[1] ETSI Caminos, Canales y Puertos - Universitad Politécnica de Madrid (UPM)
C/ Profesor Aranguren 3, 28040 Madrid, Spain
e-mail: pablo.jimenez@upm.es
[2] CEDEX Laboratorio de Geotecnia

Key words: Railway Ballast, DEM

Abstract. Some high-speed rail lines go through desert zones where sand particles transported by winds may foul track ballast layers. This fouling can be troublesome since it increases the stiffness of the layer and reduces its capacity to absorb vibrations from the rolling stock.
We are studying this phenomenon through both laboratory and numerical experiments. In the laboratory, we performed two kinds of experiments: 9 inches triaxial tests and physical modelling in the CEDEX Track Box testing facility. The latter is a unique 1:1 model of railway track section (of dimensions 21 m $\times$5 m $\times$4 m) that has been built to model high-speed rail lines (with passenger and freight trains passing at velocities of up to 400 km/h). The laboratory experiments allowed us to measure the change of stiffness with the fouling level (represented through the void contaminant index, VCI). Numerical simulations are being performed with the Discrete Element Method, reproducing drained triaxial test conditions. Due to the considerable different size of railway ballast and sand grains, we are using idealized packings of spherical particles to study this phenomenon. We are paying particular attention to the sample size effects and are registering the evolution of the stiffness with the fouling level up to high values of VCI. The results obtained from these idealized systems will be contrasted to the laboratory experiments carried out with real railway ballast and sand.

1 INTRODUCTION

The railway track is a layered foundation made of several layers: railway ballast, compacted sub-ballast and form layer, followed by an embankment or formation soil. Railway ballast is an uniformly graded coarse granular material that is placed underneath and between track sleepers. The purpose of railway ballast is to provide drainage and structural support for the loading applied by trains. Rock type, quality, size distribution, and particle shape are among the major considerations in ballasted railway track design. Usually, the ballast is produced by crushing locally available rocks such as granite or basalt.

One of the challenges found in ballasted tracks is the fouling, *i.e.* the contamination with thinner granular materials, which increases the stiffness of the layer and can make it loose its capacity to absorb vibrations. The fouling may be caused by ballast breakdown, by the migration of subgrade particles or by the deposition of coal dust, among others. In railway lines crossing desert zones, the sand carried by the wind can foul the ballast.
In this context, the CEDEX conducted some studies to analyze the phenomenon of ballast fouling with sand [1]. These studies were mainly experimental and consisted on large triaxial tests and the measurement of track stiffness in a 1:1 scale model of a railway track built in CEDEX Track Box. In these tests, ballast was fouled with fine sand in different levels to determine its influence in the ballast mechanical properties. Both tests presented very good agreement. The study concluded that the stiffening is only noticeable at high levels of contamination and also helped to quantify the effect.
In the light of these results, we are now setting up a series of numerical simulation with the Discrete Element Method [2]. This method may help to understand the behavior of railway ballast [3, 4, 5, 6, 7, 8] or phenomena caused by the fouling [3] The purpose of this on-going work is twofold: to quantify the uncertainty of the measurements and to explain the stiffening curve that has been observed in the laboratory. The main advantage of numerical modeling is that the experiments can be massively repeated, something imposible in the laboratory because of the difficulties to handle such amount of railway ballast, the duration of the tests and the specific needs. Although some DEM models reproduce much better the complex shape of the particles with clumps [3, 5] or contact models [8], fouling phenomena need a lot of particles and considerably simplifications are necessary. In fact, the modelling of the fouling needs the inclusion of so many particles that these have to be pretty simple to make numerical experiments computationally feasible.

2 METHODOLOGY

2.1 Theoretical background

Fouling degree: several index have been proposed to quantify the degree of fouling [9]. We have used the Void Contaminant Index [10], which is defined as:

$$VCI = \frac{1+e_\mathrm{f}}{e_\mathrm{b}} \frac{G_\mathrm{b}}{G_\mathrm{f}} \frac{M_\mathrm{f}}{M_\mathrm{b}} = \frac{V_{\mathrm{f},t}}{V_{\mathrm{b},void}} \,, \tag{1}$$

being e_f, e_b the void ratios, G_f, G_b the relative gravity and M_f, M_b the masses of fouling material, f, and railway ballast, b, respectively. $V_{\mathrm{b},void}$ is the volume of the voids in the clean railway ballast and $V_{\mathrm{f},t}$ is the total volume occupied by the fouling material. Therefore the definition of VCI actually corresponds to a saturation degree, which ranges from 0 (clean ballast) to 1 (completely fouled ballast).

Mechanical behavior of clean railway ballast: if the railway ballast was supposed to be a homogeneous, isotropic and lineal elastic material, under drained triaxial testing conditions, the next relationship between deviatoric stress and axial strain would be found (after the isotropic compression of the sample):

$$\sigma_1 = E_0 \varepsilon_1 \,, \tag{2}$$

where E_0 is the Young's modulus of the material. σ_3 is assumed to not change during the application of the deviatoric load.
The linear model is useful only for low stress (or strains) levels. When this is not the case, a more advanced constitutive relationship is needed. A well-known model, which is widely used to reproduce the relationship between deviatoric stress and axial strain in drained triaxial compression tests, is the celebrated hyperbolic model [11]:

$$\sigma_1 - \sigma_3 = \frac{\varepsilon_1}{\frac{1}{E_0} + \frac{\varepsilon}{(\sigma_1 - \sigma_3)_{\text{ult}}}} \,. \tag{3}$$

The elastic tangent modulus E_0 and the ultimate deviatoric stress $(\sigma_1 - \sigma_3)_{\text{ult}}$ are the two parameters that scale this model. For small strains and constant σ_3, Eq. 2 approximates Eq. 3.

Mechanical behavior of fouled railway ballast: when the ballast is fouled with a material made of much smaller grains, because of gravity, most of the fouling material goes down and saturates the bottom of the sample, while the rest of the sample remains clean. As a result, the mechanical behavior is that of a bilayered material. A simplistic approximation to the bilayered material would be a sample of height H that is made of two layers of different materials, of heights H_1 and $H - H_1$ and whose corresponding Young's moduli are E_1 and E_2 (with $E_1 > E_2$). An elastic 1D approximation to the drained triaxial conditions, would lead to a relationship like Eq. 2, with an equivalent Young's modulus given by:

$$\frac{1}{E_{\text{eq}}} = \frac{H_1}{H}\frac{1}{E_1} + \frac{(H - H_1)}{H}\frac{1}{E_2} \,. \tag{4}$$

If the Young's modulus of a railway ballast fully saturated with sand is $E_{\text{b+f}}$ and that of the clean ballast is E_{b} and $H_1 = VCI \cdot H$, this simplistic approximation would give:

$$\frac{1}{E_{\text{eq}}} = \frac{VCI}{E_{\text{b+f}}} + \frac{(1 - VCI)}{E_{\text{b}}} \,. \tag{5}$$

Equation 5 predicts that the equivalent Youngś modulus should progressively increase from E_{b} ($VCI = 0$) to $E_{\text{b+f}}$ ($VCI = 1$), with a higher rate as $VCI \to 1$.

2.2 Laboratory experiments

Several laboratory tests were performed with real railway ballast. More details are found in [1]. Ballast grains were composed of an andesite that came from an authorized quarry for railway ballast in high speed lines in Spain. Ballast sieve sizes ranged between 25 and 60 mm, with $\text{D}_{50} = 40$ mm and a coefficient of uniformness $C_u = 1.48$. The sand used to evaluate the effects of railway ballast fouling was composed mainly by quartz, with $D_{50} = 0.4$ mm and $C_u = 1.6$. The relative density of the sand was $G_{\text{f}} = 2.65$ and it presented maximum and minimum densities of $1.64 \cdot 10^3$ and $1.44 \cdot 10^3$ kg/m^3. These values correspond to porosities of $n_{\min} = 0.37$ and $n_{\max} = 0.46$.

2.2.1 Triaxial testing

The mechanical behavior of the fouled ballast was studied through large triaxial testing. Clean and fouled specimens were tested (with corresponding VCIs of 0.0, 0.15, 0.30, 0.45, 0.62, 0.80 and 1.00). This was done by pouring a certain weight of of sand into the cell containing the ballast. The sand went down and filled the void from the bottom of the specimen. The dimensions of the cell were 230 mm diameter and 460 mm high. The ballast was compacted in five layers with vibratory hammer until reach a porosity of $n_{\mathrm{b}} = 0.39$. The maximum particle size in the sample was 60 mm so the ratio cell diameter to particle size was 3.85, a little below the recommended value 5.0 [12]. The confinement pressure was 150 kPa. The deviatoric vs axial strains curves were fitted with a hyperbolic model to obtain a value of the initial tangent modulus E_0 for each VCI.

2.2.2 Physical modeling

The CEDEX Track Box (CTB) is a unique physical model of high speed railway track. This 21 m long, 5 m wide and 4 m deep model allow to test, at the real scale, complete railway track sections of conventional and high speed lines for passenger and freight trains, at speeds up to 400 km/h [1]. The simulation of the effect of the approaching, passing-by and departing of a train in a test cross-section is achieved by applying loads that are adequately unphased as a function of the train velocity. Forces are applied by three pairs of servo-hydraulic actuators (each of them can apply a maximum load of 250 kN at a frequency of 50 Hz), placed on each rail and 1,5 m longitudinally separated. Two piezoelectric actuators can apply loads up to 20 kN at 300 Hz to reproduce wheel or trach defectives. The railway track response, in terms of displacements, velocities and accelerations, is collected from a great number of LVDTs, geophones, accelerometers and pressure cells installed both inside the embankment and the bed layers (ballast, sub-ballast and form layer) of the track.
Quasi-static loading tests were performed to assess the mechanical behavior of the track fouled with sand at different levels of VCI. The tangent elastic modulus was estimated from the deformations.

2.3 DEM simulation

The discrete element method [2], implemented in YADE-DEM [13][1] is used to get more insights into the stiffening of the railway ballast fouled with sand. The toy-models are made of spherical particles. The interaction between spheres is frictional-Hookean, with normal stiffness $k_n = 2E\bar{R}$ and $1/\bar{R} = 1/R_1 + 1/R_2$ (being R_1 and R_2 the radii of interacting particles). The introduction of small particles may considerably increase the computational cost of simulations since the number of particles is much larger and the critical timestep is reduced. As the computer performance is undoubtedly limited, not all VCI levels can be simulated. We have set up a simulation plan including two main stages:

[1] `https://yade-dem.org/`.

1. **Determination of the representative cell size for clean railway ballast**: the first step is the establishment of the lowest number of large spheres that have to be included in the simulation box to get accurate measurement of the parameters for the hyperbolic model. To do that, several samples of almost equal sized spheres were compressed at scaled rates to reach the confinement isotropic stress. Then a deviatoric load was applied in one of the direction while the stress was maintained in the perpendicular ones. The deviatoric strain vs axial strain curve was fitted by a least squares procedure to get the parameters for the hyperbolic model in each case. This process was repeated several times for each number of large spheres to generate a statistical sample. The confidence interval of the measured parameters are $E_o \pm \Delta E_0$ and $(\sigma_1 - \sigma_3)_{\text{ult}} \pm \Delta (\sigma_1 - \sigma_3)_{\text{ult}}$ were established -after expecting that the values follow a normal distribution- from the following equation:

$$\Delta x = t_{\alpha,\mathcal{N}-1} \frac{S_x}{\sqrt{\mathcal{N}}}\,, \tag{6}$$

where $\mathcal{N}$ is the number of tests, S_x is the squared root of the unbiased sample variance and $t_{\alpha,\mathcal{N}-1}$ is the double side t-distributed value corresponding to a confidence level α. A coefficient of variation has been defined as

$$CoV = \frac{\Delta_x}{x}\,. \tag{7}$$

CoV is expected to decrease with the number of large spheres N_{b} in the simulation box. The critical value $N_{b,\text{c}}$ is that on which boundary or other effects have no influence on the results. This will be precisely the number of large spheres that we will use in simulations with fouled samples.

2. **Triaxial testing of fouled samples:** Once $N_{b,\text{c}}$ is known, we follow the same triaxial testing procedure that we followed with clean samples. However, when the sample has been isotropically compressed and right before the application of the deviatoric load, a set of small spheres is introduced within the voids. We would desire to include as many, and as small, as possible spheres to approximate the real conditions but this is not always possible. As the large sphere to small sphere ratio increases, the number of small spheres explodes. This has been illustrated in Figure 1. These data have been obtained after assuming that the coarse fraction reaches a random close packing [14] with porosity $n = 0.36$ and that the small fraction is packed with the same porosity within the voids created by the coarse packing. The total number of spheres in the simulation will be $N_{\text{b,c}} \cdot \left(1.0 + \frac{N_{\text{f}}}{N_{\text{b}}}\right)$. Size ratios below 10.0 are undesired because small particles could block the throats between the voids. Much higher sizes ratios would make simulations unfeasible. For example, in the laboratory experiments (section 2 above), $D_{50,\text{b}}/D_{50,\text{f}} = 100$, and this means that $360,000$ small spheres should be included per each large one to reach a VCI of 1.0.

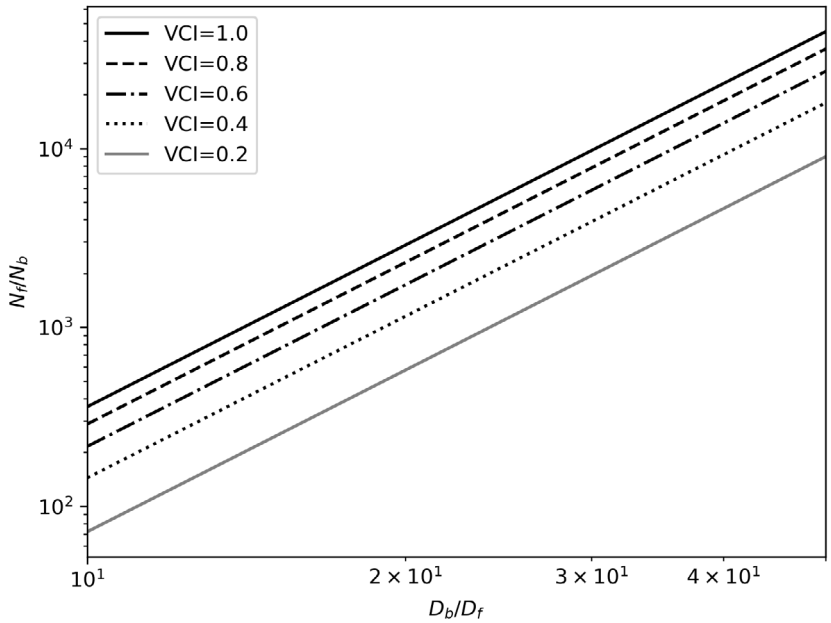

Figure 1: Number of small spheres to be included in the simulation of each large to small particle size ratio and VCI.

Table 1: Parameters used in the DEM numerical simulations to generate ensemble samples.

Mean diameter	D	0.1	m
Diameter variation	$\frac{\Delta D}{D}$	0.2	-
Young's modulus	E	$1.5 \cdot 10^7$	Pa
Particle density	ρ_{s}	$2.6 \cdot 10^3$	$\mathrm{kg.m^{-3}}$
Interparticle friction	Φ	$\pi/6$	rad
Confinment pressure	σ_3	50.0	kPa

The parameters used in the simulations are included in Table 1. Packings were generated by slowly compressing a loose cloud of particles until the confinment pressure is reached. The cell is surrounded by elastic walls, which are moved to reduce or increase the cell size and hence increase or reduce the stress. Both the size of the initial cell and the applied strain rates were scaled with $N_{\mathrm{b}}^{1/3}$ factors. The diameters of the spheres uniformly laid within the interval $D_{\mathrm{b}} \pm \Delta D_{\mathrm{b}}$. After the isotropic compression, two opposite walls were moved at constant rate until produce an axial strain of $\varepsilon_1 = 0.2$. The walls parallel to direction 1 were moved to keep the value of the confinement pressure constant.

3 RESULTS

Laboratory triaxial tests and the DEM simulation of these are showing a nonlinear deviatoric stress vs. axial strain curve that can be approximated by a hyperbolic model. In Figure 4 these curves are shown for different experiments performed with 5000 particles.

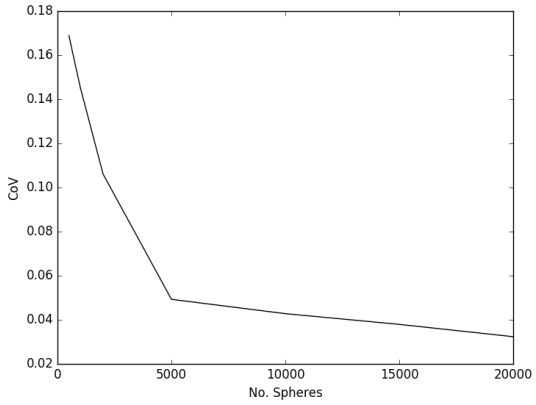

(a) Coefficient of Variation

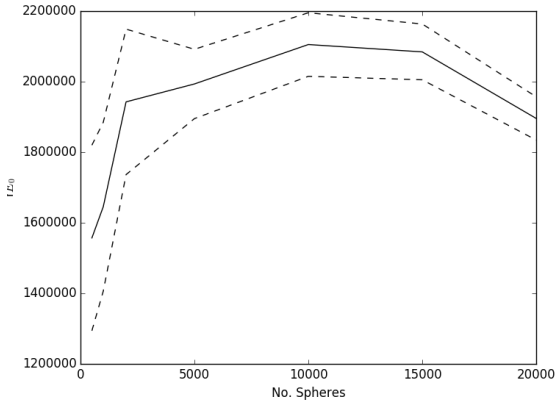

(b) Mean value and % 95 confidence interval.

Figure 2: Initial tanget modulus E_0

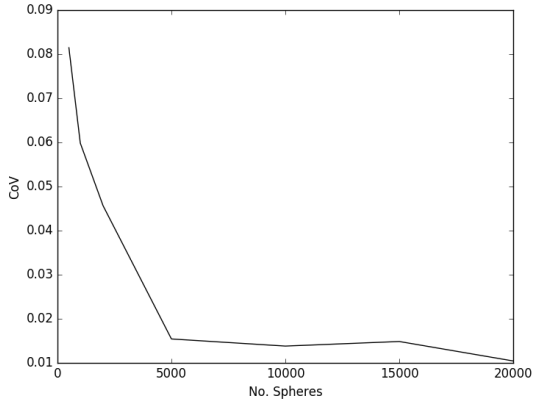

(a) Coefficient of Variation

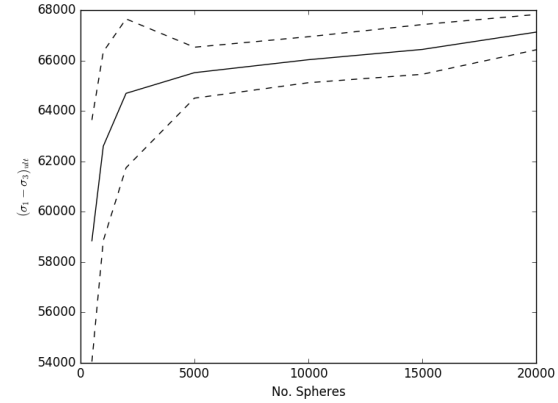

(b) Mean value and % 95 confidence interval.

Figure 3: Asymptote, $(\sigma_1 - \sigma_3)_{\text{ult}}$.

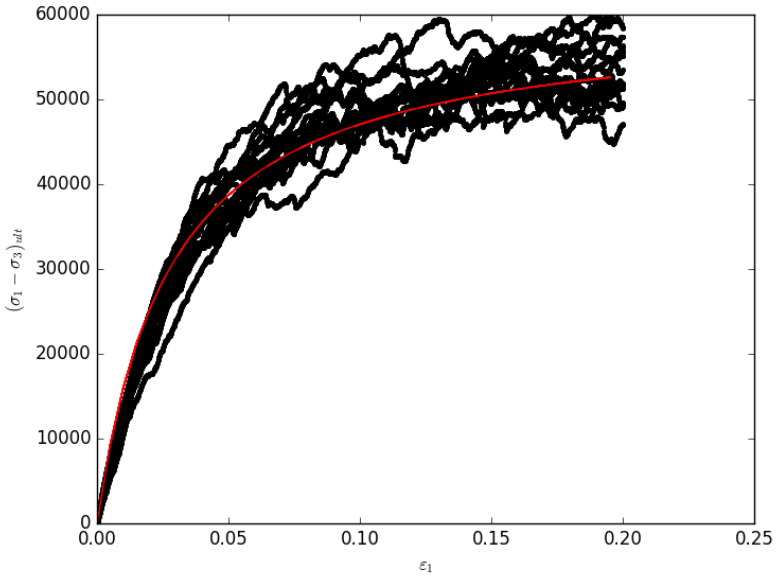

Figure 4: Deviatoric stress vs. axial strain simulated with DEM for 2000 spheres.

5000 is precisely the number that we take as $N_{\mathrm{b,c}}$, according to what is shown in Figures 2 and 3.

In Figure 5 the first values of $E_{\mathrm{b+f}}/E_{\mathrm{b}}$ obtained from DEM at low VCIs are compared to those obtained in the laboratory. A value of $D_{\mathrm{b}}/D_{\mathrm{f}} = 10$ was used. A few set of data have been produced to the date, so the uncertainty is high and conclusions cannot be yet established.

4 CONCLUDING REMARKS

- Laboratory experiments (large triaxial testing and physical 1:1 model) had shown an increase of the stiffness of railway ballast fouled with sand characterized by a bimodal behavior: no stiffening below a threshold VCI and almost linear increase over that value. However the variation of the data is considerable and the data set is reduced.

- We are investigating if an idealized DEM model made of almost uniform spherical particles contaminated with smaller spheres may help to understand how the stiffness changes at different levels of VCI. In particular we aim to understand if the curve stiffening vs VCI is actually bi-modal or not.

- The on-going DEM simulation campaign first tries to establish the confidence intervals to reduce as much as possible the number of coarse particles included in the simulation. An additional analysis on whether or not the critical number of large particles could be reduced for high VCI values will be performed.

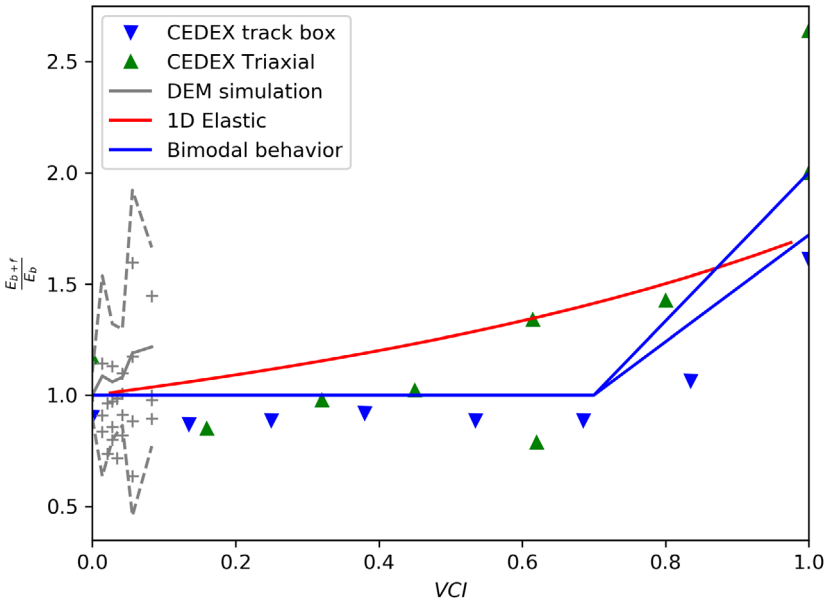

Figure 5: Stiffening as a function of the VCI.

- Once the confidence intervals are properly established, the bi-modal or continuously growing shape of the stiffening curve would be more clearly understood.

REFERENCES

[1] J. Estaire, V. Cuéllar, and M. Santana. Track stiffness in a ballast track fouled with desert. In *GEORAIL International Symposium*, 11 2017.

[2] P. A. Cundall and O. D. L. Strack. A discrete numerical model for granular assemblies. *Géotechnique*, 29(1):47–65, 1979.

[3] B. Indraratna, N. Trung Ngo, C. Rujikiatkamjorn, and J. S. Vinod. Behavior of fresh and fouled railway ballast subjected to direct shear testing: Discrete element simulation. *International Journal of Geomechanics*, 14(1):34–44, 2014.

[4] Z. Wang, G. Jing, Q. Yu, and H. Yin. Analysis of ballast direct shear tests by discrete element method under different normal stress. *Measurement*, 63.

[5] E. Mahmoud, A.T. Papagiannakis, and D. Renteria. Discrete element analysis of railway ballast under cycling loading. *Procedia Engineering*, 143:1068 – 1076, 2016. Advances in Transportation Geotechnics III.

[6] N. Trung Ngo, B. Indraratna, and C. Rujikiatkamjorn. Micromechanics-based investigation of fouled ballast using large-scale triaxial tests and discrete element modeling. *Journal of Geotechnical and Geoenvironmental Engineering*, 143(2):04016089, 2017.

[7] J. Irazábal. Numerical analysis of railway ballast behaviour using the discrete element method, 2017.

[8] J. Irazábal, F. Salazar, and E. Onate. Numerical modelling of granular materials with spherical discrete particles and the bounded rolling friction model. application to railway ballast. *Computers and geotechnics*, 85:220 – 229, 2017.

[9] B. Indraratna, L. Su, and C. Rujikiatkamjorn. A new parameter for classification and evaluation of railway ballast fouling. *Canadian Geotechnical Journal*, 48(2):322–326, 2011.

[10] N. Tennakoon, B. Indraratna, C. Rujikiatkamjorn, S. Nimbalkar, and T. Neville. The role of ballast-fouling characteristics on the drainage capacity of rail substructure. *Geotechnical Testing Journal*, 35(4):629–640, 2012.

[11] J.M. Duncan and C.Y. Chang. Nonlinear analysis of stress and strain in soils. *J. of the Soil Mech. And Found. Div*, 96:1629–1653, 1970.

[12] B. Indraratna. The effect of normal stress-friction angle relationship on the stability analysis of a rockfill dam. *Geotechnical & Geological Engineering*, 12(2):113, Jun 1994.

[13] V. Šmilauer et al. Reference manual. In *Yade Documentation 2nd ed.* The Yade Project, 2015. http://yade-dem.org/doc/.

[14] J. D. Bernal and J. Mason. Co-ordination of randomly packed spheres. *Nature*, 188:910–911, 1960.